JOURNAL OF SPACECRAFT AND ROCKETS
Vol. 40, No. 5, September–October 2003
This paper reprinted from AIAA Journal, Vol. 8, No. 5, 1970, pp. 843–851

Numerical Solution of the Hypersonic Viscous Shock-Layer Equations

R. T. DAVIS*
Virginia Polytechnic Institute, Blacksburg, Va.

Laminar flow past axisymmetric blunt bodies moving at hypersonic speeds is considered on the basis of a set of equations which govern the fully viscous shock layer for moderate to high Reynolds numbers. The shock-layer equations are derived by writing the full Navier-Stokes equations in boundary-layer coordinates and performing an order of magnitude analysis on the terms in the equations. Terms are kept up to second order in the inverse square root of the Reynolds number from both a viscous and an inviscid viewpoint, so that the simplified governing equations are uniformly valid to moderately low Reynolds numbers. To the order of the approximations involved the body surface conditions are given by slip and temperature jump conditions while a set of shock slip conditions are used to determine conditions behind the shock. The thin shock-layer approximation is then applied to the simplified set of governing equations, and the resulting equations are found to be of parabolic type. This is an important simplification as far as numerical solution of the problem is concerned since these equations can be solved by numerical methods similar to those developed for solving the boundary-layer equations. The numerical procedure consists of finding initial data at the stagnation line and then integrating downstream using an implicit finite difference method. The thin shock-layer approximation is then removed by iteration. Rather than work with the governing equations in the usual boundary-layer coordinates, it is found that it is more convenient to work with the equations in a transformed form. New dependent variables are defined by dividing the old dependent variables by their local values at the shock. In addition, a new normal independent variable is defined by dividing the old normal variable by the local distance from the body to the shock. Examples are presented to demonstrate the method and to compare with second-order boundary-layer theory.

Nomenclature

a_1 = slip constant taken to be $1.2304\ (2 - \theta_r)/\theta_r$
a^* = body nose radius of curvature
b_1 = slip constant taken to be $1.1750\ (2 - \theta_r)/\theta_r$
c_1 = slip constant taken to be $2.3071\ (2 - \alpha_t)/\alpha_t$
C_D = drag coefficient based on the local cross-sectional area, $2\ \text{Drag}/(\rho_\infty U_\infty^2 A)$
C_f = skin friction coefficient, $2\tau_w^*/(\rho_\infty^* U_\infty^{*2})$
c_p^* = specific heat at constant pressure
H = total enthalpy, H^*/U_∞^{*2}
M_∞ = freestream Mach number
n = coordinate measured normal to the body, nondimensionalized by the body nose radius
p = pressure, $p^*/(\rho_\infty^* U_\infty^{*2})$
q = heat-transfer, $q^*/(\rho_\infty^* U_\infty^{*3})$
r = radius measured from the axis of symmetry to a point on the body surface, nondimensionalized by the body nose radius
s = coordinate measured along the body surface, nondimensionalized by the body nose radius
St = Stanton number defined by equation (2.25)
T = temperature, $T = T^*/(U_\infty^{*2}/c_p^*)$
T_∞^* = freestream temperature
u = velocity component tangent to the body surface u^*/U_∞^*
U_∞^* = freestream velocity
v = velocity component normal to the body surface, v^*/U_∞^*
z = axial distance measured from the stagnation point
α = shock angle, see Fig. 1
α_t = thermal accommodation coefficient, taken to be 1
β = angle defined in Fig. 1
γ = ratio of specific heats
ϵ = perturbation parameter, $\epsilon = \left[\dfrac{\mu^*(U_\infty^{*2}/c_p^*)}{\rho_\infty^* U_\infty^* a^*}\right]$
θ_r = fraction of incident molecules diffusely reflected, taken to be 1
κ = surface curvature, nondimensionalized by the inverse of the body nose radius
μ = coefficient of viscosity, $\mu = \mu^*/\mu^*(U_\infty^{*2}/c_p^*)$
ρ = density, $\rho = \rho^*/\rho_\infty^*$
ρ_∞^* = freestream density
τ = shear stress, $\tau^*/(\rho_\infty^* U_\infty^{*2})$
ϕ = body angle defined in Fig. 1

Subscripts

w = wall value
0 = stagnation point value
sh = value behind the shock
∞ = freestream conditions

Superscripts

$-$ = quantities divided by their shock values
$*$ = dimensional quantities
j = 0 for plane flow and 1 for asixymmetric flow

Received March 3, 1969; revision received October 17, 1969. This research was initiated under NASA Grant NGR-47-004-006 and continued while the author was a summer employee of Sandia Corporation. Some of the final calculations were made with the support of Sandia Contract 48-7795. An early version of the work was presented at the AGARD Seminar on "Numerical Methods for Viscous Flows," National Physical Laboratory, Teddington, England, Sept. 18–21, 1967. The author is indebted to F. G. Blottner of Sandia Corporation for valuable advice in the development of the method of solution to the problem.

* Associate Professor of Engineering Mechanics; also Summer Employee of Sandia Corporation, Albuquerque, N. Mex. Member AIAA.

1. Introduction

THE problem of computing the hypersonic laminar flow at moderate Reynolds numbers past axisymmetric blunt bodies is an interesting one and has attracted considerable interest due to the application to re-entry problems. One may approach the problem in several ways. Two of these methods are through numerical solution of the second-order boundary-layer equations and through numerical solution of the viscous shock-layer equations.

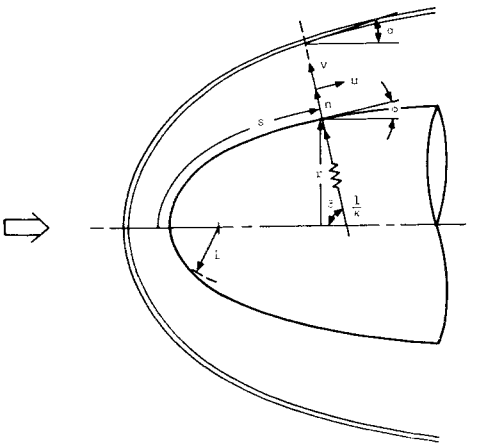

Fig. 1 Coordinate system.

The idea of using the second-order boundary-layer theory of Van Dyke[1] to compute the flowfield is appealing; however, this approach can lead to considerable difficulty. This difficulty arises for two different reasons. First, the computing time from using second-order boundary-layer theory is excessive since one must compute the inviscid flow, first-order boundary-layer flow, flow due to displacement thickness and then the second-order boundary-layer flow. Second, one can experience difficulty on long axisymmetric blunt bodies since second-order boundary-layer theory in its present form does not properly take into account the effect of strong vorticity interaction which may occur far downstream on bodies of this type. In spite of this, Davis and Flügge-Lotz[2] have developed a numerical method, based on the earlier work of Blottner and Flügge-Lotz[3] for solving the first-order boundary-layer equations, to solve the axisymmetric second-order boundary-layer equations. Fannelop and Flügge-Lotz[16] have applied essentially the same method to plane problems. This method is successful as long as one does not have problems with strong vorticity interaction, and has access to a numerical method for solving for the first-order inviscid flow and for the second-order inviscid flow which arises due to displacement thickness. Davis and Flügge-Lotz[2] and Fannelop and Flügge-Lotz[16] used an approximate method to calculate the flow due to displacement thickness; however, later Marchand, Lewis and Davis[4] and Adams[5] calculated the flow due to displacement thickness exactly, and applied the method to a number of other flow problems.

Because of the difficulties mentioned above it is desirable to seek an alternate method of approach to the problem. The most appealing method is one originally suggested by Cheng[6] (see also Cheng[15]) for solving a set of equations valid in the entire shock layer. Davis and Flügge-Lotz[2] have given a similar set of equations, but ones which contain some second-order curvature terms left out of Cheng's theory. These terms only effect the solution when γ is not close to 1. Kaiser and Flügge-Lotz[14] have shown that these curvature terms have a fairly significant influence on stagnation region shock stand-off distance and skin friction for $\gamma = 1.4$. The shock-layer equations contain all of the terms in the Navier-Stokes equations which contribute to second-order boundary-layer theory for arbitrary γ plus those which arise to second order in the outer inviscid flow. By making the thin shock-layer approximation on the resulting momentum equation normal to the body surface, these equations are reduced to a set of equations which are parabolic and can thus be solved numerically in a manner similar to the method of Blottner and Flügge-Lotz[3] for solving the first-order boundary-layer equations. This approximation is removed by iterating on the normal momentum equation which includes the neglected terms. Fast convergence is achieved since γ is close to one.

Cheng's[6] equations are applicable to either the direct or inverse problem. However, he applied the method to only the inverse problem so that better accuracy could be gained. The method presented here is applied to the direct problem only and determines the shock shape if the body shape is given. The method is fast in terms of computer time and avoids the difficulty of strong vorticity interaction encountered in second-order boundary-layer theory.

We choose here to consider only the axisymmetric problem; however, the plane problem can be handled in exactly the same manner. We consider only the case of a perfect gas; however, no difficulties should be encountered in extending the method to chemically reacting flows.

The method to be discussed here is similar in idea, but represents a vast improvement in the method developed by Davis and Chyu[7] and Chen.[8]

2. Formulation of the Problem

The compressible Navier-Stokes equations are written in a boundary-layer coordinate system (see Fig. 1) and nondimensionalized (see Nomenclature) by variables which are of order one in the region near the body surface (boundary layer) for large Reynolds numbers. This set of equations and variables are given by Van Dyke.[1] The same set of equations are then written in variables which are of order one in the essentially inviscid region outside the boundary layer. Terms in each set of equations are kept up to second-order in the inverse square root of a Reynolds number. A comparison of the two sets of equations is then made and one set of equations is found from them which is valid to second order in both the outer and inner regions. A solution to this set of equations is thus uniformly valid to second-order in the entire shock layer for arbitrary γ.

The shock-layer equations obtained from keeping terms up to second order are of a hyperbolic-parabolic nature. If terms were kept up to third or higher order, the equations would be elliptic and thus very difficult to solve numerically.

A final approximation is made to the shock-layer equations by making the thin shock-layer approximation to the normal momentum equation. The purpose of this approximation is to make the equations totally parabolic. This final set of equations can then be solved by numerical methods similar to methods used in boundary-layer theory. An iteration method will be used to remove this approximation.

A more detailed discussion of the shock-layer equations can be found in a paper by Davis and Flügge-Lotz.[2] Weinbaum[9] has discussed the same set of equations, but applied to the near wake problem.

The viscous shock-layer equations are given by the following:

continuity equation

$$[(r + n\cos\phi)^j \rho u]_s + [(1 + \kappa n)(r + n\cos\phi)^j \rho v]_n = 0 \quad (2.1)$$

s momentum equation

$$\rho\{u[u_s/(1 + \kappa n)] + vu_n + [\kappa/(1 + \kappa n)]uv\} + p_s/(1 + \kappa n) = [\epsilon^2/(1 + \kappa n)^2(r + n\cos\phi)^j] \times [(1 + \kappa n)^2(r + n\cos\phi)^j\tau]_n \quad (2.2a)$$

where

$$\tau = \mu[u_n - \kappa u/(1 + \kappa n)] \quad (2.2b)$$

n momentum equation

$$\rho\{u[v_s/(1 + \kappa n)] + vv_n - [\kappa/(1 + \kappa n)]u^2\} + p_n = 0 \quad (2.3a)$$

where with the thin shock-layer approximation this Eq. (2.3a) becomes

$$p_n = [\kappa/(1 + \kappa n)]\rho u^2 \quad (2.3b)$$

energy equation

$$\rho\{u[T_s/(1+\kappa n)] + vT_n\} - \{u[p_s/(1+\kappa n)] + vp_n\} = [\epsilon^2/(1+\kappa n)(r+n\cos\phi)^j][(1+\kappa n)(r+n\cos\phi)^j q]_n + (\epsilon^2/\mu)\tau^2 \quad (2.4a)$$

where

$$q = (\mu/\sigma)T_n \quad (2.4b)$$

equation of state

$$p = [(\gamma-1)/\gamma]\rho T \quad (2.5)$$

and viscosity law

$$\mu = (1+c')/(T+c')(T)^{3/2} \quad (2.6a)$$

where

$$c' = c^*/(\gamma-1)M_\infty{}^2T_\infty{}^* \quad (2.6b)$$

c^* is taken to be 198.6°R for air.

Consistent with the approximations used in the above set of equations the boundary conditions are given as below. Slip at the body surface is a second-order effect and is thus included here, we also consider the case of shock slip even though it is a third-order effect.

The conditions at the body surface are given by (see Fig. 1) the following:

surface conditions

$$v = 0 \quad (2.7a)$$

$$\left.\begin{aligned} u &= \epsilon^2 a_1(1/p)\{[(\gamma-1)/\gamma]T\}^{1/2}\tau \quad (2.7b)\\ p &= p_w + \epsilon^2 b_1(\sigma/T)\{[(\gamma-1)/\gamma]T\}^{1/2}q \quad (2.7c)\\ T &= T_w + \epsilon^2 c_1(\sigma/p)\{[(\gamma-1)/\gamma]T\}^{1/2}q \quad (2.7d)\end{aligned}\right\} \text{ at } n = 0$$

In the above a_1, b_1, and c_1 are constants (see Shidlovskiy[10] and Nomenclature) and the subscript w refers to the body surface. The above boundary conditions can be modified to include mass injection at the boundary. Equation (2.7c) is not used as a boundary condition, but is needed to obtain the surface pressure.

The conditions at the shock including slip are given by (see Fig. 1),

shock conditions

$$u_{sh} = u'_{sh}\sin(\alpha+\beta) + v'_{sh}\cos(\alpha+\beta) \quad (2.8a)$$

$$v_{sh} = -u'_{sh}\cos(\alpha+\beta) + v'_{sh}\sin(\alpha+\beta) \quad (2.8b)$$

where u'_{sh} and v'_{sh} are the components of velocity tangent and normal to the shock interface, respectively, and are given along with temperature, pressure, and density from the following expressions:

$$\rho_{sh}v'_{sh} = -\sin\alpha \quad (2.8c)$$

$$\epsilon^2\mu_{sh}(u'_n)_{sh} + \sin\alpha u'_{sh} = \sin\alpha\cos\alpha \quad (2.8d)$$

$$\epsilon^2\sigma^{-1}\mu_{sh}(T_n)_{sh} + \sin\alpha T_{sh} - (\sin\alpha/2)(u'_{sh}-\cos\alpha)^2 = \sin\alpha/2\{[4\gamma/(\gamma+1)^2]\sin^2\alpha + [2/(\gamma-1) - 4(\gamma-1)/(\gamma+1)^2]\,1/M_\infty{}^2 - 4/(\gamma+1)^2M_\infty{}^4\sin^2\alpha\} \quad (2.8e)$$

$$p_{sh} = [2/(\gamma+1)]\sin^2\alpha - (\gamma-1)/\gamma(\gamma+1)M_\infty{}^2 \quad (2.8f)$$

$$\rho_{sh} = \gamma P_{sh}/(\gamma-1)T_{sh} \quad (2.8g)$$

The angles used in the shock conditions are shown in Fig. 1. Primes used with u_{sh} and v_{sh} denote components evaluated tangent and normal to the shock interface, respectively. All other quantities used in the boundary conditions and governing equations are as defined in the Nomenclature. The conditions given are slightly different from those of Cheng[6,15] and Bush[17] in that they have been modified to give the exact shock relations for finite Mach number when slip is not present.

If one examines Eqs. (2.1–2.6), it is found that the equations are parabolic if Eq. (2.3b) is used for the normal pressure gradient. These equations are quite similar to the compressible boundary-layer equations.

For ease in numerical computation a different form of Eqs. (2.1–2.6) is used. This is done in the case of the independent normal variable in order to have a constant number of steps in the finite difference grid between the body and the shock. This eliminates interpolation to determine the shock position and eliminates the problem of adding grid points in the normal direction as the computation proceeds downstream from the stagnation point. The transformation is also important as far as the iteration method to determine the shock position is concerned. This will be discussed later. We also define new dependent variables by dividing the old dependent variables by their local values at the shock. The new dependent variables thus have the value one at the shock.

The new independent and dependent variables are defined by

$$\eta = n/n_{sh} \quad (2.9a)$$

$$\xi = s \quad (2.9b)$$

$$\bar{u} = u/u_{sh} \quad (2.9c)$$

$$\bar{v} = v/v_{sh} \quad (2.9d)$$

$$\bar{t} = T/T_{sh} \quad (2.9e)$$

$$\bar{p} = p/p_{sh} \quad (2.9f)$$

$$\bar{\rho} = \rho/\rho_{sh} \quad (2.9g)$$

$$\bar{\mu} = \mu/\mu_{sh} \quad (2.9h)$$

The differential relations needed to transform Eqs. (2.1–2.6) are given by

$$\partial/\partial s = \partial/\partial\xi - \eta(n'_{sh}/n_{sh})(\partial/\partial\eta) \quad (2.10a)$$

$$\partial/\partial n = (1/n_{sh})\,\partial/\partial\eta \quad (2.10b)$$

$$\partial^2/\partial n^2 = (1/n^2_{sh})\,\partial^2/\partial\eta^2 \quad (2.10c)$$

where

$$n'_{sh} = dn_{sh}/d\xi$$

The s momentum and energy Eq. (2.2a and 2.4a) written in the transformed ξ, η plane can be written in the standard form for a parabolic equation as

$$\partial^2 w/\partial\eta^2 + \alpha_1(\partial w/\partial\eta) + \alpha_2 w + \alpha_3 + \alpha_4(\partial w/\partial\xi) = 0 \quad (2.11)$$

where w equals $\bar{u}$ for the s momentum equation, and $\bar{t}$ for the energy equation. The coefficients $\alpha_1 - \alpha_4$ can be written as follows:

s momentum equation

$$\alpha_1 = \frac{\rho_{sh}u_{sh}n'_{sh}}{\epsilon^2\mu_{sh}}\frac{n_{sh}}{1+\kappa n_{sh}\eta}\frac{\bar{\rho}\bar{u}\eta}{\bar{\mu}} - \frac{\rho_{sh}v_{sh}n_{sh}}{\epsilon^2\mu_{sh}}\frac{\bar{\rho}\bar{v}}{\bar{\mu}} + \frac{\bar{\mu}_n}{\bar{\mu}} + \frac{\kappa n_{sh}}{1+\kappa n_{sh}\eta} + \frac{\cos\phi n_{sh}}{r+n_{sh}\eta\cos\phi} \quad (2.12a)$$

$$\alpha_2 = -\frac{\rho_{sh}u'_{sh}n_{sh}}{\epsilon^2\mu_{sh}}\frac{n_{sh}}{1+\kappa n_{sh}\eta}\frac{\bar{\rho}\bar{u}}{\bar{\mu}} - \frac{\rho_{sh}v_{sh}n_{sh}}{\epsilon^2\mu_{sh}}\frac{\kappa n_{sh}}{1+\kappa n_{sh}\eta}\frac{\bar{\rho}\bar{v}}{\bar{\mu}} - \kappa\frac{n_{sh}}{1+\kappa n_{sh}\eta}\frac{\bar{\mu}_\eta}{\bar{\mu}} - \left(\frac{\kappa n_{sh}}{1+\kappa n_{sh}\eta} + \frac{\cos\phi n_{sh}}{r+n_{sh}\eta\cos\phi}\right)\times\frac{\kappa n_{sh}}{1+\kappa n_{sh}\eta} \quad (2.12b)$$

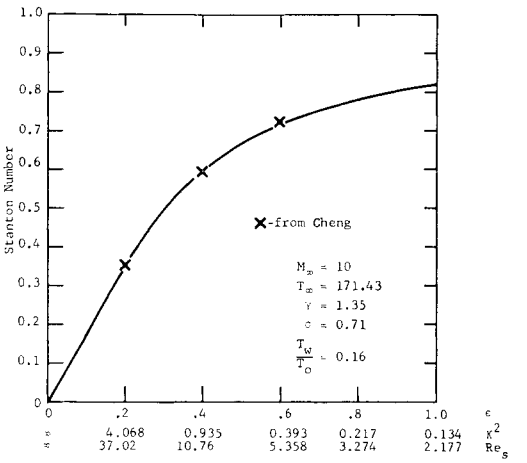

Fig. 2 Comparison of present results with those of Cheng.[13]

$$\alpha_3 = -\frac{p_{sh}n_{sh}}{\epsilon^2\mu_{sh}}\frac{n_{sh}}{1+\kappa n_{sh}\eta}\frac{1}{\bar\mu}\frac{1}{u_{sh}}\left(\bar p_\xi - \frac{n'_{sh}}{n_{sh}}\eta\bar p_\eta + \frac{p'_{sh}}{p_{sh}}\bar p\right) \quad (2.12c)$$

$$\alpha_4 = -(\rho_{sh}u_{sh}n_{sh}/\epsilon^2\mu_{sh})(n_{sh}/1+\kappa n_{sh}\eta)\,\bar\rho\bar u/\bar\mu \quad (2.12d)$$

energy equation

$$\alpha_1 = \frac{\rho_{sh}u_{sh}n'_{sh}\sigma}{\epsilon^2\mu_{sh}}\frac{n_{sh}}{1+\kappa n_{sh}\eta}\frac{\bar\rho\bar u\eta}{\bar\mu} - \frac{\rho_{sh}v_{sh}n_{sh}\sigma}{\epsilon^2\mu_{sh}}\frac{\bar\rho\bar v}{\bar\mu} + \frac{\bar\mu_\eta}{\bar\mu} + \frac{\kappa n_{sh}}{1+\kappa n_{sh}\eta} + \frac{\cos\phi n_{sh}}{r+n_{sh}\eta\cos\phi} \quad (2.13a)$$

$$\alpha_2 = -(\rho_{sh}u_{sh}T'_{sh}\sigma/\epsilon^2\mu_{sh}T_{sh})(n_{sh}/1+\kappa n_{sh}\eta) + \bar\rho\bar u/\bar\mu \quad (2.13b)$$

$$\alpha_3 = \frac{p_{sh}u_{sh}n_{sh}\sigma}{\epsilon^2\mu_{sh}T_{sh}}\frac{1}{\bar\mu}\left[\frac{n_{sh}\bar u}{1+\kappa n_{sh}\eta}\left(\bar p_\xi - \frac{n'_{sh}}{n_{sh}}\eta\bar p_\eta + \frac{p'_{sh}}{p_{sh}}\bar p\right) + \frac{v_{sh}}{u_{sh}}\bar v\bar p_\eta\right] + \frac{u_{sh}^2\sigma}{T_{sh}}\left(\bar u_\eta - \frac{\kappa n_{sh}}{1+\kappa n_{sh}\eta}\bar u\right)^2 \quad (2.13c)$$

$$\alpha_4 = -(\rho_{sh}u_{sh}n_{sh}\sigma/\epsilon^2\mu_{sh})(n_{sh}/1+\kappa n_{sh}\eta)\,\bar\rho\bar u/\bar\mu \quad (2.13d)$$

The remaining equations are written as follows:
continuity equation

$$[n_{sh}(r+n_{sh}\eta\cos\phi)\rho_{sh}u_{sh}\bar\rho\bar u]_\xi + [(r+n_{sh}\eta\cos\phi)\times\{(1+\kappa n_{sh}\eta)\rho_{sh}v_{sh}\bar\rho\bar v - n'_{sh}\rho_{sh}u_{sh}\bar\rho\bar u\eta\}]_\eta = 0 \quad (2.14)$$

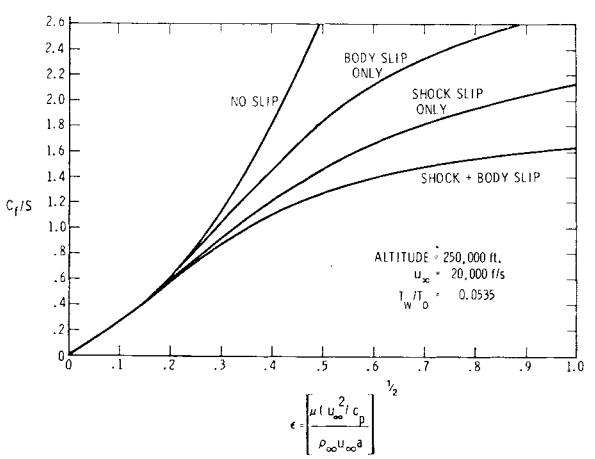

Fig. 3 Skin friction in the stagnation region as a function of ϵ.

n momentum equation

$$\frac{\bar\rho\bar u}{1+\kappa n_{sh}\eta}\left(\bar v_\xi - \frac{n'_{sh}}{n_{sh}}\eta\bar v_\eta + \frac{v'_{sh}}{v_{sh}}\bar v\right) + \frac{v_{sh}}{u_{sh}}\frac{\bar\rho\bar v}{n_{sh}}\bar v_\eta - \frac{\kappa}{1+\kappa n_{sh}\eta}\frac{u_{sh}}{v_{sh}}\bar\rho\bar u^2 + \frac{p_{sh}}{\rho_{sh}u_{sh}v_{sh}n_{sh}}\bar p_\eta = 0 \quad (2.15a)$$

where with the thin shock-layer approximation this equation becomes

$$\bar p_\eta = (\kappa/1+\kappa n_{sh}\eta)(\rho_{sh}u^2{}_{sh}n_{sh}/p_{sh})\,\bar\rho\bar u^2 \quad (2.15b)$$

equation of state

$$\bar p = \bar\rho\bar t \quad (2.16)$$

viscosity law

$$\bar\mu = [(T_{sh}+c')/(T_{sh}\bar t + c')]\bar t^{3/2} \quad (2.17)$$

where c' is as defined in Eq. (2.6b).

The boundary conditions become:
surface conditions

$$\left.\begin{aligned}\bar v &= 0 && (2.18a)\\ \bar u &= \epsilon^2 a_1(\mu_{sh}/n_{sh}p_{sh}\bar p)\{[(\gamma-1)/\gamma]\times T_{sh}\bar t\}^{1/2}\,\bar\mu(\bar u_\eta - \kappa n_{sh}\bar u) && (2.18b)\\ \bar t &= \bar t_w + \epsilon^2 c_1(\mu_{sh}/n_{sh}p_{sh}\bar p)\{[(\gamma-1)/\gamma]T_{sh}\bar t\}^{1/2}\,\bar\mu\bar t_\eta && (2.18c)\end{aligned}\right\} \text{ at } \eta = 0$$

conditions at the shock

$$\bar u = \bar v = \bar t = \bar p = \bar\rho = \bar\mu = 1 \quad \text{at } \eta = 1 \quad (2.19a\text{–}f)$$

The shock conditions are now involved in the governing Eqs. (2.11–2.15) and are obtained from Eqs. (2.8a–g). In the above Eqs. (2.12–2.15) $(\ )'$ means $d(\ )/d\xi$, which should not be confused with the primes in Eqs. (2.8) which are defined differently.

An equation of mass conservation can be obtained from Eq. (2.14) by integrating from $\eta = 0$ (the body) to $\eta = 1$ (the shock) while holding ξ constant. This results in

$$dm/d\xi = (r+n_{sh}\cos\phi)[n'_{sh}\rho_{sh}u_{sh} - (1+\kappa n_{sh})\rho_{sh}v_{sh}] \quad (2.20)$$

where

$$m = \int_0^1 n_{sh}(r+n_{sh}\eta\cos\phi)\rho_{sh}u_{sh}\bar\rho\bar u d\eta \quad (2.21)$$

is proportional to the rate of mass flux between the body and shock at a given position on the body surface.

Equations (2.20) and (2.21) will be used to determine the shock location in the numerical method which determines the flowfield.

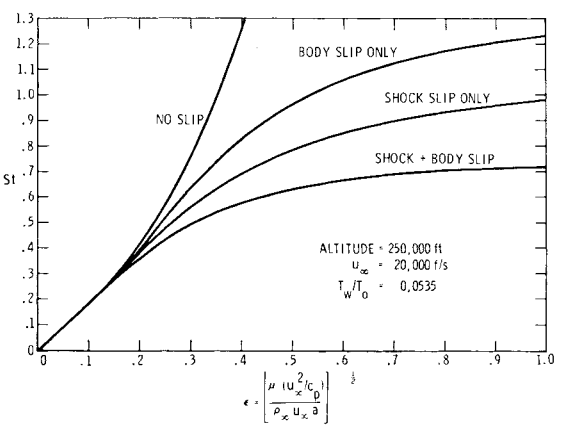

Fig. 4 Stanton number in the stagnation region as a function of ϵ.

The dimensionless shear stress, heat transfer and wall pressure (see Nomenclature) are given by

$$C_f = 2\epsilon^2(\mu_{sh}u_{sh}/n_{sh})\bar{\mu}[(\partial\bar{u}/\partial\eta) - \kappa n_{sh}\bar{u}] \quad (2.22)$$

$$q_w = -\epsilon^2(\mu_{sh}T_{sh}/n_{sh}\sigma)\bar{\mu}\partial\bar{t}/\partial\eta - \epsilon^2(\mu_{sh}u^2{}_{sh}/n_{sh})\bar{\mu}\bar{u}\partial\bar{u}/\partial\eta \quad \text{at } \eta = 0 \quad (2.23)$$

and

$$p_w = p - \epsilon^2 b_1\mu_{sh}/n_{sh}\bar{t} \times \{[(\gamma - 1)/\gamma]T_{sh}\bar{t}\}^{1/2}\bar{\mu}\bar{t}\eta \quad (2.24)$$

while the Stanton number is defined as

$$St = q_w/(H_0 - H_w) \quad (2.25)$$

The second term in Eq. (2.23) is a term which arises only in slip flow and is due to sliding friction (see Maslen[11]). If wall injection is present in slip flow, additional terms arise in these shear stress and heat-transfer expressions.

3. Solutions in the Stagnation Region

The governing Eqs. (2.11–2.17) reduce to ordinary differential equations in the stagnation region if Eq. (2.15b) is used for the normal pressure gradient. This can be done by expanding the shock conditions (2.8a–g) in power series. If Eq. (2.15b) is used for the normal momentum equation, no truncation of the series is required and the series can be integrated term by term indicating that the equations are parabolic. There is a difficulty with the boundary conditions, however. This can be demonstrated as follows. Assume a power series for the shock shape in the form

$$n_{sh} = n_{sh_1} + s^2 n_{sh_2} + \ldots \quad (3.1)$$

Using this relation in Eq. (2.8a) for u_{sh} along with Eq. (2.8c–g) and simplifying we can find an expression for u_{sh} in terms of a power series. For simplicity we consider here only the no slip case. The first term in the series is of the form

$$u_{sh} = \{1 - [2/(\gamma + 1)][1 - 1/M_\infty{}^2] \times 2n_{sh_2}/(1 + n_{sh_1})\}\, s + \ldots \quad (3.2)$$

A similar expression results for the pressure behind the shock. This is given by

$$p_{sh} = \frac{2}{\gamma + 1} - \frac{\gamma - 1}{\gamma(\gamma + 1)M_\infty{}^2} - \frac{2}{\gamma + 1} \times \left(1 - \frac{2n_{sh_2}}{1 + n_{sh_1}}\right)^2 s^2 + \ldots \quad (3.3)$$

v_{sh}', T_{sh}, and ρ_{sh} do not involve n_{sh_2} in the first terms of their expansions.

The difficulty mentioned is that n_{sh_2} cannot be determined from the stagnation region equations. It is a quantity that depends upon the flow downstream. We must therefore assume a value for n_{sh_2}. The usual assumption is to assume that it is zero. In order to find stagnation region solutions we do this, but later we show how this assumption can be removed. It will be shown that the assumption that $n_{sh_2} = 0$ is included in the assumption of local similarity and can result in an error of about 20%. The influence of the downstream shock shape on the solution has the effect of making the problem elliptic rather than parabolic. Fortunately, in some cases the problem is so weakly elliptic that the elliptic nature of the boundary conditions can be overcome by iteration. It may be possible to treat n_{sh_2} as an initial condition and determine it from the condition that the solution proceed downstream. This possibility has not been explored.

Figures (2–9) are the results obtained from solving the governing equations in the stagnation region. These results will be discussed later. The next section will deal with the method of solution of the equations.

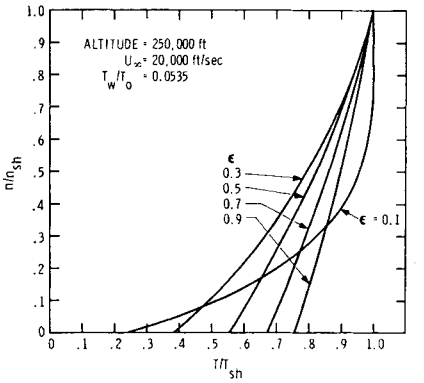

Fig. 6 Temperature profiles in the stagnation region.

4. Method of Solution

In this section we discuss the method of solution of the problem. The problem basically reduces to the solution of parabolic partial differential equations. There are many ways to solve this type of equation. The method that will be used here is similar to the method that Blottner and Flügge-Lotz[3] developed for solving the boundary-layer equations. This method has been shown to be stable and accurate. A few modifications have been made to the method to solve the present problem. Below we will give a brief discussion of the application of this method to the present problem.

The derivatives in Eq. (2.11) are replaced with finite difference quotients. In order to handle high Reynolds number cases we allow for variable grid spacing in the η direction so that we can use many points in the region near the body surface where the variables are changing rapidly. Let the subscript m denote the station measured along the body surface and n denote the station measured normal to the body surface. It can then be shown by Taylor series expansions that

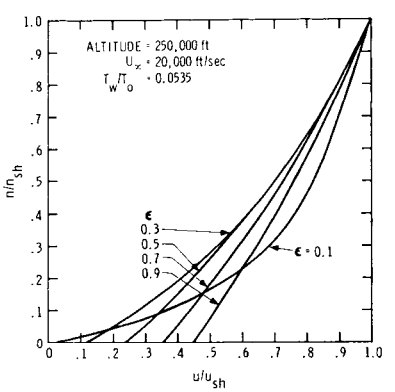

Fig. 5 Velocity profiles tangent to the body surface in the stagnation region.

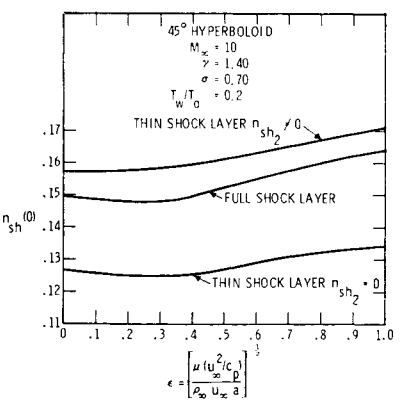

Fig. 7 Shock stand-off distance in the stagnation region as a function of ϵ.

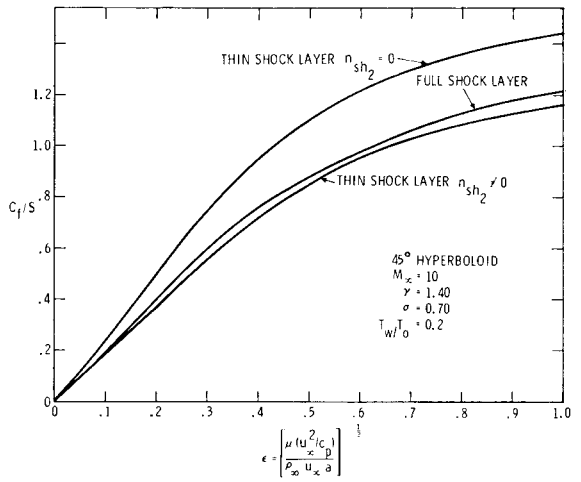

Fig. 8 Skin friction in the stagnation region as a function of ϵ.

central differences taken in the η direction at the point m,n are

$$(\partial w/\partial n)_{m,n} = [\Delta\eta_{n-1}/\Delta\eta_n(\Delta\eta_n + \Delta\eta_{n-1})]w_{m,n+1} + [(\Delta\eta_n - \Delta\eta_{n-1})/\Delta\eta_n\Delta\eta_{n-1}]w_{m,n} - [\Delta\eta_n/\Delta\eta_{n-1}(\Delta\eta_n + \Delta\eta_{n-1})]w_{m,n-1} - \tfrac{1}{6}(\partial^3 w/\partial\eta^3)_{m,n}\Delta\eta_n\Delta\eta_{n-1} \quad (4.1)$$

$$(\partial^2 w/\partial\eta^2)_{m,n} = [2/\Delta\eta_n(\Delta\eta_n + \Delta\eta_{n-1})]w_{m,n+1} - (2/\Delta\eta_n\Delta\eta_{n-1})w_{m,n} + [2/\Delta\eta_{n-1}(\Delta\eta_n + \Delta\eta_{n-1})]w_{m,n-1} - \tfrac{1}{12}(\partial^4 w/\partial\eta^4)_{m,n}\Delta\eta_n\Delta\eta_{n-1} - \tfrac{1}{3}(\partial^3 w/\partial\eta^3)_{m,n}(\Delta\eta_n - \Delta\eta_{n-1}) - \tfrac{1}{12}(\partial^4 w/\partial\eta^4)_{m,n}(\Delta\eta_n - \Delta\eta_{n-1})^2 \quad (4.2)$$

The subscript n on a step increment denotes the step from the nth to the n plus first point.

The derivative in the ξ direction in Eq. (2.11) is handled in the usual way as a two-point difference. If the derivative $\partial w/\partial\xi$ is evaluated at the midpoint $(m - \frac{1}{2}, n)$ and the other terms are averaged we obtain the Crank-Nicolson scheme. If a backward difference is used for $\partial w/\partial\xi$ at the point (m,n) and all other quantities are evaluated at (m,n) also we obtain a purely implicit scheme. The implicit method is more stable than the Crank-Nicolson scheme; however, it was found that in the present problem both schemes were stable as long as shock slip was not included. When shock slip was

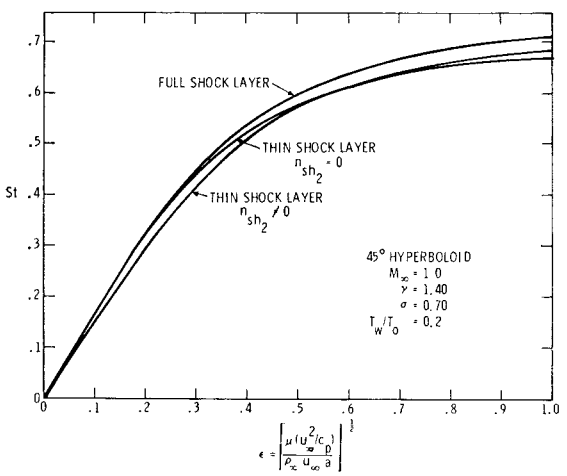

Fig. 9 Stanton number in the stagnation region as a function of ϵ.

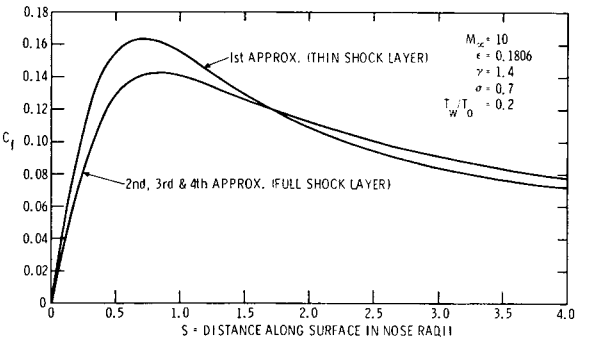

Fig. 10 Skin friction on a 45° hyperboloid.

included it was found that the Crank-Nicolson method could become unstable. This was probably due to the way in which the shock slip was handled. The truncation errors in the ξ direction in the Crank-Nicolson scheme are smaller $[0(\Delta\xi)^2]$ than those in the implicit scheme $[0(\Delta\xi)]$, therefore one would expect more accurate results from the Crank-Nicolson scheme for a given step size $\Delta\xi$. The numerical results do not show much difference, however, between the two methods for a given step size $\Delta\xi$. Experiments were run to demonstrate convergence as $\Delta\eta$ and $\Delta\xi$ go to zero.

When the difference quotients are substituted into the differential Eq. (2.11) a difference equation of the following form results.

$$A_n W_{n-1} + B_n W_n + C_n W_{n+1} = D \quad (4.3)$$

The solution to this equation is straightforward once the boundary conditions are given. For the method of solution one is referred to Richtmyer.[12] The boundary conditions at the wall are given by writing the slip conditions Eqs. (2.18b) or (2.18c) in three point forward difference form. Manipulation of this equation, Eq. (4.3), and the equation for the solution to the problem allows one to determine a condition to satisfy the wall conditions. The condition at the shock is given by $W = 1$; however, the shock conditions now appear as unknown coefficients in the Eqs. (2.12) or (2.13).

The method of solution is then as follows. Start at the stagnation-point where $\partial w/\partial\xi = 0$. Equation (2.11) then reduces to an ordinary differential equation. Care must be taken to evaluate the pressure gradient term properly in the stagnation region. This can be done by series expansion. Make initial guesses for all of the flow profiles. Integrate, using the finite difference method, the energy Eqs. (2.11 and 2.13). Now evaluate all quantities related to temperature such as viscosity. Next, integrate, in the same manner, the s momentum Eqs. (2.11 and 2.12) to determine a $\bar{u}$ velocity profile. Next integrate the continuity Eq. (2.14) to determine first the shock stand-off distance from Eq. (2.21) and then the $\bar{v}$ component of velocity from Eq. (2.14). In the stagnation region these equations must also be handled with series expansions. Finally integrate Eq. (2.15) to determine

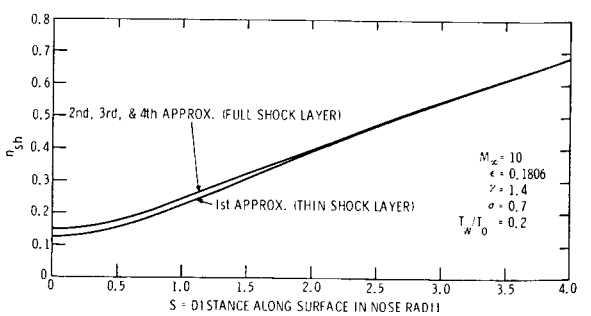

Fig. 11 Shock stand-off distance on a 45° hyperboloid.

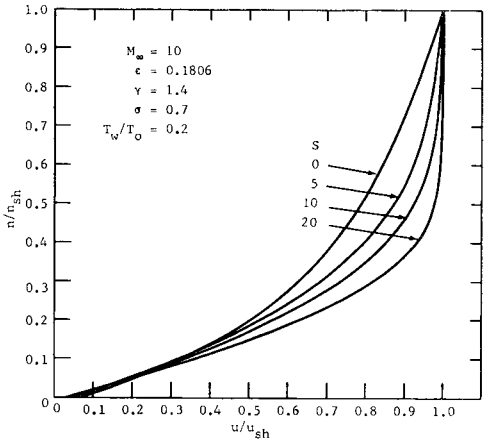

Fig. 12 Velocity profiles tangent to the body surface of a 45° hyperboloid.

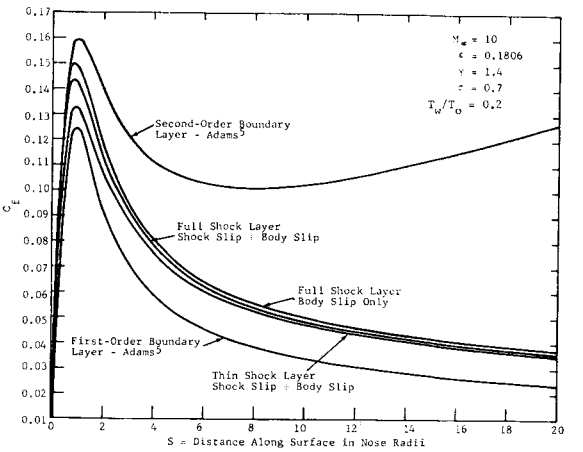

Fig. 14 Skin friction on a 45° hyperboloid.

the pressure. Evaluate the coefficients in the equations using the shock conditions Eq. (2.8) and the new value of n_{sh}. Repeat the above steps until the solution converges. Then step along the body surface and iterate at each step if necessary. The previous values of the profiles are used at each new step as a first guess. It was found that there was very little change after the second iteration at each step except at the stagnation point where more iterations are needed.

In the first approximation we assume that n'_{sh} is equal to zero at each step on the body surface. We also use Eq. (2.15b) in the first approximation. We will call this approximation the thin shock-layer approximation, and solutions obtained using this approximation will be labeled thin shock-layer in the figures. In the second approximation, we use n'_{sh} calculated from the stand-off distance in the first approximation. We also use the $\bar{v}$ terms calculated in the first approximation to approximate the $\bar{v}$ terms in Eq. (2.15a) in the second approximation. Further iterations are performed until the solution converges. Converged solutions of this type will be labeled full shock layer in the figures. These approximations on n'_{sh} and the $\bar{v}$ terms in the normal momentum equation are necessary in order to make the equations parabolic.

The shock-slip conditions Eq. (2.8) were handled by simply evaluating the $(u'_n)_{sh}$ and $(T_n)_{sh}$ terms from the previous step in the iteration and then solving the resulting equations for the shock conditions. This was found to converge even for fairly small values of Reynolds number.

The option of using variable grid spacing in the η direction helps in high Reynolds number or cold wall cases. The computer program contains the variable spacing option, which has been used with success in decreasing the computation time while attaining high accuracy. If one looks at the truncation error terms in the η direction in Eq. (2.11) using Eqs. (4.1) and (4.2) one finds that they are

$$\text{relative truncation error} = \{\tfrac{1}{12}\Delta\eta_n\Delta\eta_{n-1}[(\partial^4 w/\partial\eta^4) + 2\alpha_1(\partial^3 w/\partial\eta^3)]_{m,n} + \tfrac{1}{3}(\Delta\eta_n - \Delta\eta_{n-1}) \times (\partial^3 w/\partial\eta^3)_{m,n}\}/[(\partial^2 w/\partial\eta^2) + \alpha_1(\partial w/\partial\eta)]_{m,n} \quad (4.4)$$

We have neglected the last term in Eq. (4.2) since it will be small. From a constant step size calculation we can calculate the terms in the brackets. Then by setting the relative truncation error equal to a constant we can calculate the grid spacing $\Delta\eta_n$ that would produce the desired truncation error. Using this new step size distribution we can then recalculate a solution which, for the same number of steps in η, should be much more accurate. A calculation of this type done at the stagnation point can save considerable computing time for a computation that goes far downstream. A method could be devised for changing the grid spacing as we go downstream also; however, in the present program the grid spacing determined at the stagnation point is used at every downstream station.

5. Discussion of Results

As a check on the method of solution, stagnation region solutions were calculated to compare with some of the results of Cheng.[13] Cheng gives extensive results but only a few points are shown to point out the agreement that is obtained. Identical flow conditions were assumed. The results are shown in Fig. 2 for Stanton number. Even though the equations are slightly different from Cheng's, one sees that the results are almost identical. The K^2 parameter is a parameter defined by Cheng[13] and Re_s is the Reynolds number behind the shock on the stagnation streamline. The characteristic

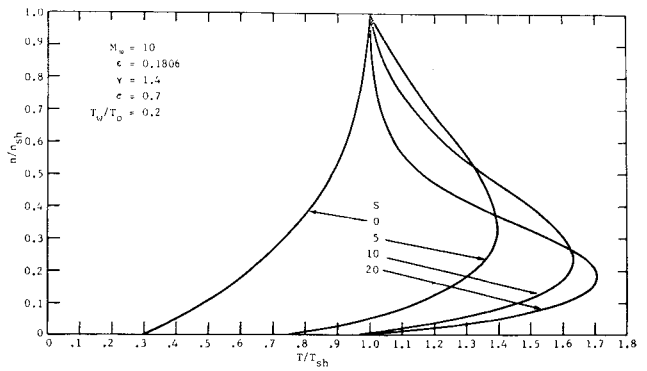

Fig. 13 Temperature profiles normal to a 45° hyperboloid surface.

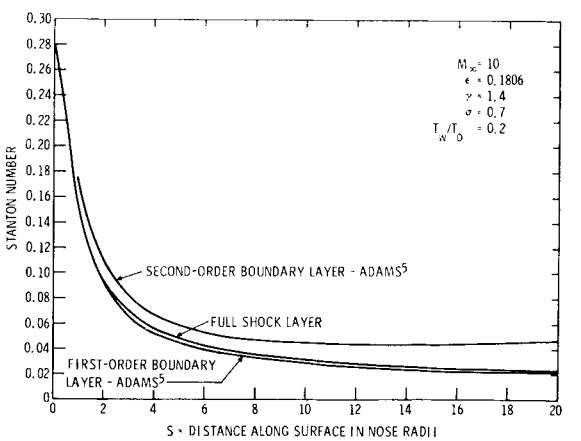

Fig. 15 Stanton number on a 45° hyperboloid.

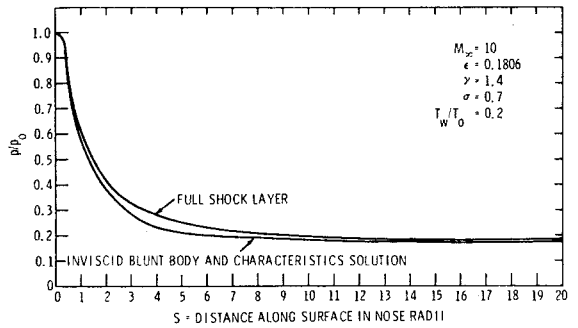

Fig. 16 Pressure distribution on a 45° hyperboloid.

length taken in the shock Reynolds number is the body nose radius. The term n_{sh_2} in Eq. (3.1) is taken to be zero and the thin shock-layer approximation is made on the normal momentum equation in the calculations. The influence of these assumptions will be shown later.

Figures (3–6) are stagnation line results for a typical flow situation. Again n_{sh_2} is taken to be zero. The freestream conditions were taken to be standard atmospheric conditions at 250,000 ft with a freestream velocity of 20,000 fps. Prandtl number σ is taken to be 0.7, the ratio of specific heats γ is taken to be 1.4, and Sutherland's viscosity law is used. If the body nose radius of curvature is chosen to be one inch, then ϵ turns out to be 0.224.

The results shown in Figs. 3 and 4 indicate that for low Reynolds numbers, shock and body slip are large effects, in fact above values of ϵ of about 0.2, they should not be neglected. These two figures also give some indication of the range of validity of second-order boundary-layer theory. For both skin friction and Stanton number, second-order boundary-layer theory predicts an increase over first-order theory, therefore, these curves should show an upward curvature initially as they do. The trend has already reversed at around an ϵ of about 0.3, so second-order boundary-layer theory appears to only be valid to an ϵ of about 0.2. If one looks at Figs. 5 and 6 one notices that this is about the value of ϵ when the viscous layer extends from the body to the shock. One would not expect that even higher order boundary-layer theory would be valid when there is no distinct boundary-layer or outer inviscid flow. The velocity and temperature profiles shown in Figs. 5 and 6 are for the case when both shock slip and body slip are included.

A typical case was chosen to compare the present results with second-order boundary-layer theory. Complete second-order calculations have been made by Adams[5] for flow over a hyperboloid which is asymptotic to a cone of 45° total interior angle. For purposes of comparison the same flow conditions, viscosity law, etc. were chosen here. Freestream Mach number M_∞ is 10.0, ϵ is 0.1806, Prandtl number σ is 0.70, and the ratio of specific heats γ is 1.40. The ratio of wall to inviscid stagnation point temperature is taken to be 0.2. Shock and body slip are included in all calculations.

Figures 7–9 indicate the effect of various approximations at the stagnation point. Figures 10 and 11 show the solutions for one particular value of ϵ at points along the body surface. In the first approximation n'_{sh} is taken to be zero at every point along the body surface and the $\bar{v}$ terms are neglected in the normal momentum Eq. (2.15a). The lower curve in Fig. 7 shows the stand-off distance at the stagnation point as a function of ϵ with these approximations. Figure 11 shows the distribution of n_{sh} along the body surface for one particular value of ϵ. The values of n'_{sh} and $\bar{v}$ calculated from this approximation are put back into the equations and the equations are integrated again resulting in a new solution. In subsequent iterations the previous calculated values of the quantities n'_{sh} and $\bar{v}$ are used. As is shown in Figs. 10 and 11 the convergence is achieved in two steps. This is due to the fact that γ is close to one. There is very little difference in the results in further iterations as the figures show. These results are also a good check of the assumption of local similarity at the stagnation point. The effect of n'_{sh} being taken equal to zero represents an error of about 20% in itself at the stagnation point in calculating skin friction as is shown in Fig. 8. This is found by comparing the two thin shock-layer calculations, one including the effect of n'_{sh}, the other not. The effect is not as pronounced on other flow quantities such as Stanton number shown in Fig. 9. Kaiser and Flügge-Lotz[14] have found similar results for flow past a sphere in using the method of series truncation. It is interesting to note that the shock stand-off distance at the stagnation point converges to the exact inviscid value as ϵ goes to zero (i.e., Reynolds number goes to infinity). The value obtained at Arnold Engineering Development Center (AEDC) from an inviscid blunt-body solution using the Lomax Ames program gives a value of 0.1498 for the stagnation point shock stand-off distance under identical freestream conditions. Figure 7 shows that a value very close to this is being approached as ϵ goes to zero. Other flowfield quantities show similar correct trends.

One reason that the method works so well is that the shock stand-off distance in the first approximation is quite close to the final result and therefore the n'_{sh} value calculated from the first approximation is quite accurate. Figure 11 indicates this and also shows that the stand-off distance does not change after the second iteration.

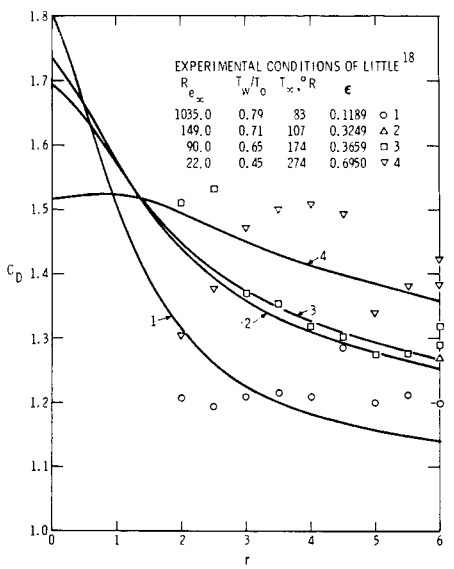

Fig. 17 Drag coefficient for a 90° hyperboloid.

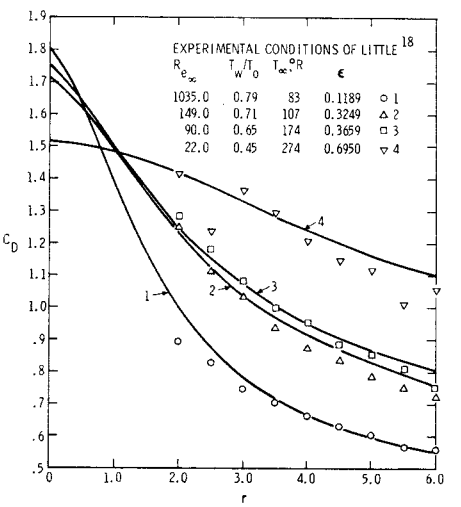

Fig. 18 Drag coefficient for a 45° hyperboloid.

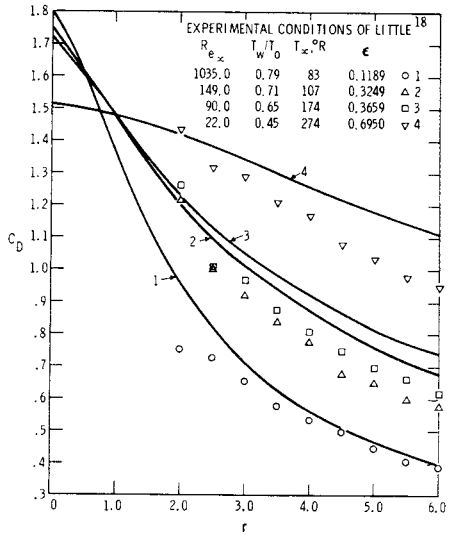

Fig. 19 Drag coefficient for a 20° hyperboloid.

Figures 12 and 13 show velocity and temperature profiles at various stations along the body surface. These were obtained from the second iteration. One sees clearly how the linear type velocity profile is swallowed up as the outer flow becomes an inviscid cone type flow.

Second-order boundary-layer theory gives erroneous results when applied to a problem of this type. Figure 14 shows the result of applying second-order boundary-layer theory to the problem. The effect of strong vorticity interaction is not taken care of properly by second-order boundary-layer theory. Figures 15 and 16 show similar comparisons for Stanton number and surface pressure.

Figures 17–19 show a comparison of results obtained from the present method with experimental results obtained by Little.[18] The test cases were for a range of shock Reynolds numbers resulting in different values of ϵ and for flows over hyperboloid shaped bodies of various lengths opening to asymptotic total interior angles of 90°, 45°, and 20°. The numerical calculations were performed including both shock and body slip.

Little[18] has mentioned that some of the data for the 90° hyperboloid cases is not applicable to the present calculations, especially for the short bodies, since the bodies were not long enough for the flow to reach a supersonic condition before the base of the body was reached, This should explain the scatter in the data for this case. The same type of scatter is not present in the other cases and the data seems to follow a definite trend. Use of values of θ_r and α_t in the slip conditions other than one would reduce the drag and would make the calculations agree better with the experiments. Little estimates his possible experimental error in drag at plus or minus seven percent. In general, the calculations fall within these error bounds.

6. Conclusion

A method has been discussed for solving the viscous shock layer eqs. (2.1–2.8) which are valid for arbitrary γ but moderate to high shock Reynolds numbers. Comparison with the experimental results of Little[18] indicates that the method gives reasonable results to much lower values of Reynolds number than one would expect. Comparison with Cheng[6] indicates good agreement even for a value of γ of 1.4 and one would thus generally consider the effect of the curvature terms to be negligible for most engineering applications.

References

[1] Van Dyke, M., "A Review and Extension of Second-Order Hypersonic Boundary-Layer Theory," *Rarefied Gas Dynamics, Fluid Symposium Supplement 2*, edited by J. A. Lauermann, Vol. II, Academic Press, New York, 1963.

[2] Davis, R. T. and Flügge-Lotz, I., "Second-Order Boundary-Layer Effects in Hypersonic Flow Past Axisymmetric Blunt Bodies," *Journal of Fluid Mechanics*, Vol. 20, Pt. 4, 1964, pp. 593–623.

[3] Blottner, F. G. and Flügge-Lotz, I., "Finite-Difference Computation of the Boundary-Layer with Displacement Thickness Interaction," *Journal de Mecanique*, Vol. II, No. 4, 1963.

[4] Marchand, E. O., Lewis, C. H., and Davis, R. T., "Second-Order Boundary-Layer Effects on a Slender Blunt Cone at Hypersonic Conditions," AIAA Paper 68-54, New York, 1968.

[5] Adams, J. C., "Higher Order Boundary-Layer Effects on Analytic Bodies of Revolution," TR-68-57, 1968, Arnold Engineering Development Center.

[6] Cheng, H. K., "The Blunt-Body Problem in Hypersonic Flow at Low Reynolds Number," Rept. AF-1285-A-10, 1963, Cornell Aeronautical Lab.

[7] Davis, R. T. and Chyu, W. J., "Laminar Flow Past A Sphere at High Mach Number," *Journal of Fluid Mechanics*, Vol. 24, Pt. 3, 1966, pp. 481–495.

[8] Chen, C. H., "Laminar Flow Past Axisymmetric Blunt Bodies at High Mach Number and Moderate Reynolds Number," Ph.D. dissertation, 1967, Virginia Polytechnic Institute.

[9] Weinbaum, S., "Near Wake Uniqueness and a Re-Examination of the Throat Concept in Laminar Mixing Theory," AIAA Paper 67-65, New York, 1967.

[10] Shidlovskiy, V. P., *Introduction to Dynamics of Rarefied Gases*, American Elsevier, New York, 1967.

[11] Maslen, S. H., "On Heat Transfer in Slip Flow," *The Journal of Aerospace Sciences*, Vol. 25, No. 6, June 1958, pp. 400–401.

[12] Richtmyer, R. D., *Difference Methods for Initial-Value Problems*, Interscience, New York, 1957.

[13] Cheng, H. K., "Hypersonic Shock-Layer Theory of the Stagnation Region at Low Reynolds Number," *1961 Heat Transfer and Fluid Mechanics Institute*, Stanford Press, Stanford, Calif., 1961.

[14] Kaiser, J. E. and Flügge-Lotz, I., "Viscous Hypersonic Flow Around a Blunt Body," TR 178, 1968, Division of Engineering Mechanics, Stanford Univ.

[15] Cheng, H. K., "Viscous Hypersonic Blunt-Body Problems and the Newtonian Theory," *Fundamental Phenomena in Hypersonic Flow*, edited by J. G. Hall, Cornell Univ. Press, Ithaca, N.Y., 1966, pp. 90–132.

[16] Fannelop, T. K. and Flügge-Lotz, I., "Viscous Hypersonic Flow Over Simple Blunt Bodies Including Second-Order Effects," *Journal de Mecanique*, Vol. 5, 1966, pp. 69–100.

[17] Bush, W. B., "On the Viscous Hypersonic Blunt Body Problem," *Journal of Fluid Mechanics*, Vol. 20, Pt. 3, 1964, pp. 353–367.

[18] Little, H. R., "An Experimental Investigation of Surface Conditions on Hyperboloids and Paraboloids at a Mach Number of 10," M.S. thesis, 1969, Univ. of Tennessee.